ADITUM

Journal of Oncology and Cancer Screening

Open Access Research Article

Comparing antibacterial activities of CuO/ZnO nanocomposite growing on crystalline and amorphous silica extracting from bagasse ash

Yirgalem Negash, Birhanu Tolosa, Tegene Bantewesen and Gebisa Bekele*

Department of Material Science and Engineering, Adama Science and Technology University, 1888 Adama, Ethiopia.

Article Info

Received: July 09, 2021
Accepted: July 15, 2021
Published: July 22, 2021

***Corresponding author:** Gebisa Bekele, Department of Material Science and Engineering, Adama Science and Technology University, 1888 Adama, Ethiopia.

Citation: Yirgalem Negash, Birhanu Tolosa, Tegene Bantewesen and Gebisa Bekele. (2021) " Comparing antibacterial activities of CuO/ZnO nanocomposite growing on crystalline and amorphous silica extracting from bagasse ash", J Oncology and Cancer Screening, 3(1); DOI: http;//doi.org/07.2021/1.1034.

Abstract

Copper Oxide-Zinc oxides (CuO/ZnO) nanocomposite with supporting materials is becoming a better antibacterial agent because of low agglomeration, low electron hole recombination and stability in the solution. In this work, we investigated the nature of the supporting materials on the antibacterial activities of CuO/ZnO nanocomposites. Three samples: CuO/ZnO bare, amorphous and crystalline silica supported CuO/ZnO nanocomposite were synthesized by sol-gel method, and then the antibacterial activities of three nanocomposites have compared on gram-negative (E.coli) and gram-positive (S. aureus) bacteria. The calculated crystal sizes from XRD data are 16.3 nm for CuO/ZnO bare, 12.5 nm for amorphous silica supported CuO/ZnO and 29.1 nm for crystalline silica supported CuO/ZnO. In addition, this, the hairy like structure of CuO/ZnO nanocomposite were seen on amorphous silica supported CuO/ZnO by using SEM. When antibacterial activities of three nanocomposites were tested by using the agar diffusion method, amorphous silica supported CuO/ZnO showed inhibition zone of 59.1% for S. aureus and 63% for E.coli compared with CuO/ZnO bare, also 57% for S.ureus and 60% for E.coli compared with Crystalline silica supported CuO/ZnO. Therefore, amorphous silica supporting CuO/ZnO nanocomposite is a promising antibacterial agent.

Key Words: bagasse ash; amorphous; crystalline; and antibacterial agent

1. Introduction:

Nano-scaled materials gained enormous attention from the research communities for different applications due to their fascinating and remarkable properties such as their durability, high diffusivity, and versatile chemical and biological activities [1]. Some of the applications of nano-scaled materials are cosmetics, paints, displays, batteries, medicine, catalysis, energy, construction, microelectronic circuit fabrication, piezoelectric devices, fuel cell, and solar cell [2],[3],[4].Especially, due to antibiotic resistance microorganisms/bacteria have been come into view, tremendous works have been reported for using nano-scaled material as antibacterial agent [5]. Nano-scaled materials are mostly metal oxide semiconductor including ZnO, [6] CuO, [7] WO_3 [8], MgO, [9] TiO_2 [9] and Fe_2O_3 [10]. The main challenges in using these materials fully as antibacterial agents are the following: (i) high recombination rate of photogenerated electrons and holes, (ii) high agglomeration formation, (iii) large bandgap (i.e. for TiO_2 and ZnO), and (iv) instability in aqueous solution.Tariq Jan et.al reported that coupling CuO with ZnO reduces the recombination rate by separating photoelectron electrons and holes so that antibacterial activities of the nanocomposite was significantly enhanced [11].SongfaQiu et.al also synthesized mesoporous silica supported CuO/ZnO to reduce the agglomeration and instability issues and then they showed that antibacterial activities of mesoporous silica supported CuZnO were much better comparing with mesoporous silica supported CuO and ZnO because of Cu doped ZnO have smaller band gap than ZnO so that doped ZnO can be activated by irradiation of visible light and mesoporous silica reduce agglomeration and instability of the composite in the solution [11].Here, the effect of nature of the supporting materials (i.e. silica) on antibacterial activities of the CuO/ZnOnanocomposite has not investigated yet. Hence, in this work, we investigated the effect of the nature of the silica substrate that is amorphous and crystalline silica on the antibacterial activities of CuO/ZnO nanocomposite because amorphous and crystalline silica have different surface properties that modify the properties CuO/ZnO nanocomposite. Both amorphous and

crystalline silica were extracted from Bagasse ash by simple and effective sol-gel method. Three samples such as bare CuO/ZnO, amorphous silica supported and crystalline silica supported CuO/ZnO were synthesized in this work, and thentheir antibacterial activities were tested by agar well diffusion method. It was found that the antibacterial activities of amorphous silica supported CuO/ZnO were better than the two rest previously mentioned samples because of porous nature of amorphous silica facilitate large and dispersed growth of CuO/ZnO nanocomposite as confirmed by SEM.

2. Methodology:

2.1. Materials:

In this research the raw materials consist of Sugarcane bagasse ash (SBA) obtained from Wonji Shewa Sugar Factory (ETHIOPIA), Zinc(II) acetate dihydrate ($Zn(CH_3COO)_2.2H_2O$) 98% (Merck), copper(II) sulfate pentahydrate ($CuSO_4.5H_2O$) 98%(Merck), ethanol 98%, sodium hydroxide (NaOH) (Merck), filter paper, ethylene glycol ($(CH_2OH)_2$), citric acid 10% ($C_6H_8O_7$), Hydrochloric acid (HCl), dimethylsulfoxide (DMSO) and distilled (DI) water. Chemicals used in this experiment were analytical grade and used without extra purification.

2.2. Extraction of amorphous silica and crystalline silica from sugar cane bagasse ash:

The sugar cane bagasse ash (SCBA) was calcined in the furnace for 3hrs at 600 °C to remove carbon. Then it cooled down up to reach room temperature before taking it out. Following that, the ash was washed with 1M HCl to remove extractive minerals and iron composition. The cleaned products were filtered with filter paper what-man No 41. Then 20g filtrated solid was treated with 200mL of NaOH 3M under heating and stirring at 100 °C for 90 minutes. The mixture was cooled and filtered to remove solid residues. The obtained sodium silicate solution was precipitated using a 1M HCl solution until pH 7 and kept for 24hrs at 25 ºC for silica to completely solidify. The slurry was filtered and washed with DI water continual until it reached neutral PH. The solid was dried using an oven at 100 °C for 24 hrs [12]. The same techniques conducted for extraction of crystalline silica except calcination temperature, 1100 °C used in this case [13].

2.3. Synthesis of CuO/ZnO bare:

50 ml of distilled water,50 ml of ethylene glycol,12.3g of citric acid and 10.649 g of Zn $(CH_3COO)_2.2H_2O$ added to the baker followed by vigorously steering for 1 hrs at room temperature. Then 2.66 g of $CuSO_4.5H_2O$ which dissolved in 25ml DI water was added drop by drop and stirred at 60ºC for 3hrs.It was placed in a dark area for 48 hrs. After that washed with DI water several times and followed by ethanol. Finally, the gel dried at 120ºC followed by calcination at 500ºC for 4hrs [14].

2.4. Synthesis of CuO/ZnO loaded on amorphous silica and crystalline silica:

2g of amorphous silica added to 50 ml of DI water, 50 ml of ethylene glycol and 12.3g of citric acid followed by stirring for 30 minutes at room temperature. Then 10.649 g of Zn $(CH_3COO)_2.2H_2O$ dissolved in 25 ml of DI water added drop by drop and stirred vigorously for 1 hrs at room temperature. After that 2.66g of $CuSO_4.5H_2O$which dissolved in 25ml DI water was added drop by drop and stirred at 60ºC for 3hrs. It was placed in a dark area for 48 hrs. After that washed with DI water several times and followed by ethanol. Finally, the gel dried at 120ºC followed by calcination at 500ºC for 4hrs.The synthesis of CuO/ZnO loaded on crystalline silica followed the same procedure except crystalline silica used in this case.

3. Results and Discussions:

3.1. XRD Analysis:

XRD patterns of amorphous silica, crystalline silica, CuO/ZnO bare, amorphous silica supported CuO/ZnO and crystalline silica supported CuO/ZnO g are showed in Fig 1.As shown in this figure, the amorphous silica show broad width single peak at 24° that shows no regular arrangement of atoms and the crystalline silica showed narrow width of peak revealing that there is regular arrangement of atoms. As mentioned previously, to obtain amorphous silica, the bagasse ash was calcinated at 600 °C whereas to obtain crystalline silica; it was calinated at 1100 °C. Thus, this indicates that the amorphous silica transformed to crystalline silica as calcination temperature exceeded the calcination temperature at which amorphous silica was formed. As shown in Fig.1, the diffraction peaks of CuO/ZnO bare were found at angles $2\theta=34.2^{\circ},35.7^{\circ},37^{\circ},38.9^{\circ},41.7^{\circ},48.7^{\circ},53.8^{\circ},58.4^{\circ},61.5^{\circ}$ and corresponding miller indices of (hkl) = (110), (002), $(11\bar{1})$, (111), (200), $(20\bar{1})$, (020), (202), $(11\bar{3})$. The diffraction angle 38.9° and 37° which corresponding to the indices (111) and $(11\bar{1})$ respectively was peak of CuO while compared with the inbuilt data's of JCPDS card no.450937 [15]. And then, the rest listed angles were corresponding to the peaks of ZnO. This confirmed that the nanocomposite consists of both metal oxides. The diffraction peaks of the amorphous silica supported CuO/ZnO and crystalline silica supported CuO/ZnOs are also shown in Fig.1. The diffraction peak corresponding to the CuO/ZnO in amorphous silica supported CuO/ZnO nano composite is insignificant. This may be due to the amorphous nature of silica that is its porosities were affecting the x-ray scattering by the loaded composite materials [16]. In fact, the presence of the CuO/ZnO on the amorphous silica was confirmed by EDX, which will be discussed in next section. However, for the diffraction pattern of crystalline silica supported CuO/ZnO, the peak of the crystalline silica reduced significantly while the peaks of the CuO/ZnO nanocomposite intensively appeared due to the surface of crystalline silica covered by nanocomposite and scattering from the CuO/ZnO nanocomposite was not interrupted by nature of silica. The crystalline sizes were calculated from 2θ and FWHM of the (hkl) peaks using Scherer's equation.

$$D = k\lambda / \beta \cos\theta \ldots\ldots\ldots\ldots\ldots\ldots\ldots\ldots\ldots\ldots (1)$$

Where, D is Crystallite size, K is Shape factor has a typical value of about 0.9,

λ is the X-ray wavelength with value 1.54060nm, β is the line broadening at half the maximum intensity (FWHM), **θ** is the Bragg angle. It was calculated that the average crystallite sizes of the nano-composite are less than 50 nm, for instance, the average crystallite sizes are 16.3 nm for CuO/ZnO bare, 29.1nm for crystalline silica supported CuO/ZnO and 12.5nm for amorphous

silica supported CuO/ZnO. The reasons why the crystalline sizes were calculated are due to the crystalline sizes have significant effect on the performance of the nano-scaled semiconductor materials. Tanaka, K reported that as particles size reduced, the photocatalytic activities of the nano-scaled metal oxide semiconductor was enhanced. Therefore, here in this work, it is important to consider the particle sizes of our synthesized composites materials.

3.2. FT-IR Analysis:

The FTIR spectroscopy spectra of CuO/ZnO bare, amorphous silica supported CuO/ZnO and crystalline silica supported CuO/ZnO were shown in Fig 2. The IR spectra of the three samples were recorded under the infrared spectroscopy of wavenumber of 500–4000cm$^{-1.}$ Broad absorption peaks at between 3280–3650cm−1 were observed for the three nanocomposites. The presence of -OH functional group indicates the existence of water absorbed on the surface of nanocomposite. The C=O functional group observed at the wave number 1629cm^{-1} for CuO/ZnO bare ,1620cm-1 for amorphous silica supported CuO/ZnO and 1660cm^{-1} for crystalline silica supported CuO/ZnO. The absorption peaks in the region between 1100cm^{-1} -1200 cm^{-1} shows the presence of strong C-O bonds in a nanocomposite. An intense peak ascribed to the stretching at 2924 cm^{-1} for the three nanocomposites indicates the C-H functional group. The peaks of Si-O-Si were observed at 1090cm^{-1} and 1120cm^{-1} for amorphous silica supported CuO/ZnO and crystalline silica supported CuO/ZnO respectively. The absorption bands of metal oxide were below 1000cm^{-1}, this is due to their inter-atomic vibrations [18]. We confirmed that Strong absorption band in the range 700 to 400 cm^{-1} assigned to Cu-O stretching mode [19].

Generally for ZnO (stretching of Zn-O) was between 400cm^{-1} and 531cm^{-1} which confirmed the wurtiz structure [20].For our case we obtained the absorption peak on 476cm^{-1},460cm^{-1} and 482cm^{-1} for CuO/ZnO loaded on amorphous silica, CuO/ZnO loaded on crystalline silica and CuO/ZnO bare nanocomposite. The peaks show the presence for ZnO (stretching Zn-O) of the nanocomposite synthesized by sol-gel method. The absorption peak observed at 606cm^{-1},476cm^{-1} and 681cm^{-1} were indicating that the presence of Cu-O stretching on CuO/ZnO bare, CuO/ZnO loaded on amorphous silica and CuO/ZnO loaded on crystalline silica respectively.

3.3. SEM-EDX Analysis:

The Scanning electrons microscopy (SEM) and Energy dispersion x-ray (EDX) spectroscopy of the CuO/ZnO bare, amorphous silica supported CuO/ZnO and crystalline silica supported CuO/ZnO were shown in Fig 3.As seen from Fig 1(a), the CuO/ZnO bare show high agglomeration because as size of the particle scale-down the surface areas increases which leads higher surface energy of the nanocomposite increases proportionally. Thus, minimize this energy, the nano-scaled composite agglomerate which hinders the antibacterial activities of the CuO/ZnO nanocomposite. The agglomeration properties of the nonocomposite were not observed in amorphous silica supported CuO/ZnO and crystalline silica supported CuO/ZnO nanocomposites because in both cases silica acts as supporting and dispersing agents as shown in Fig 1(b) and (C). Comparing to crystalline silica supported CuO/ZnO, amorphous silica supported CuO/ZnO nanocomposite shows hairy like growth of the CuO/ZnO nanocomposite. As shown from the EDX graph, all required metals are appeared, but Mo is impurity that may come from source of silica.

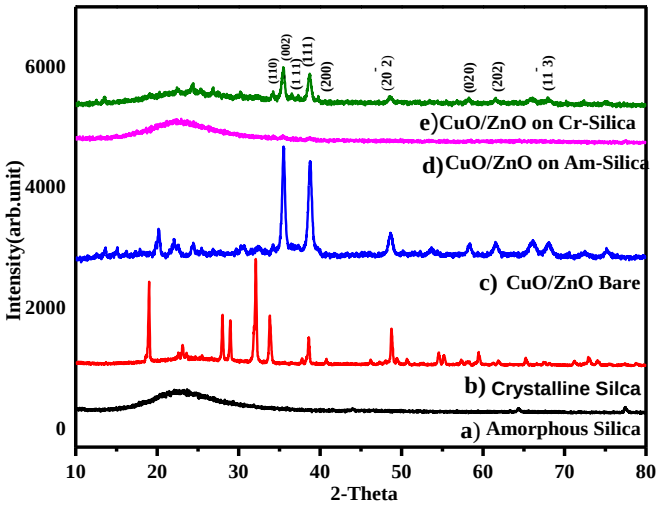

Figure 1: XRD pattern of a) amorphous silica, b) crystalline silica, c), CuO/ZnO bare, d), amorphous silica supported CuO/ZnO and e) crystalline silica supported CuO/ZnO.

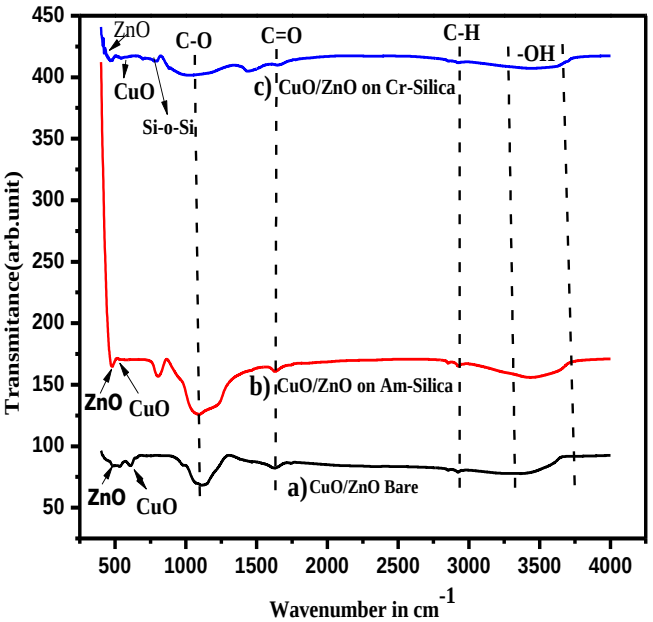

Figure 2: FT-IR spectra of a) CuO/ZnO bare, b), CuO/ZnO loaded on amorphous silica and c) CuO/ZnO loaded on crystalline silica.

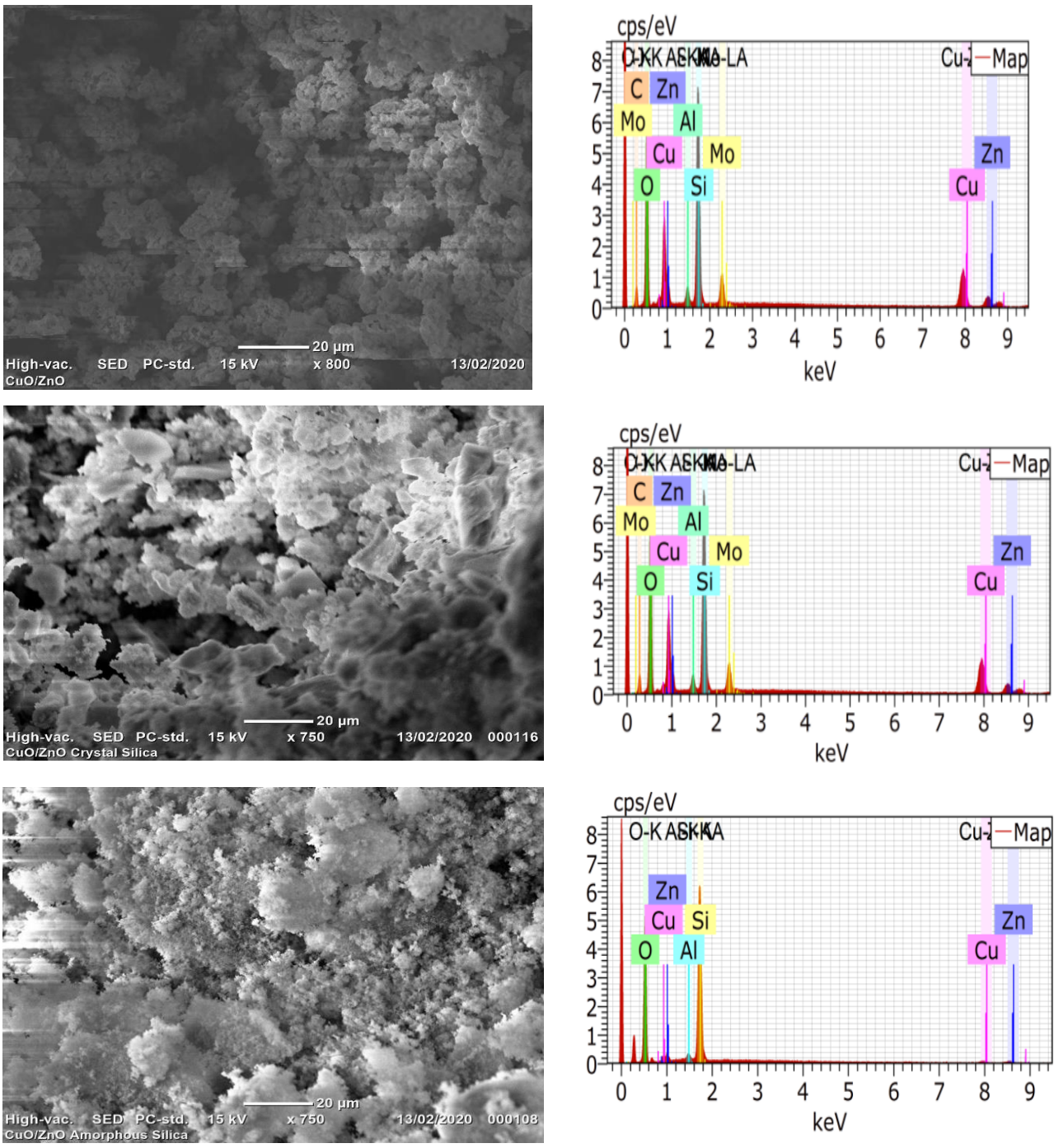

Figure 3: SEM-EDX of a) CuO/ZnO bare, b) CuO/ZnO loaded on crystalline silica and c) CuO/ZnO loaded on amorphous silica

3.4 Antibacterial activities test:

The antibacterial test was conducted on both gram negative (E. coli) bacteria and gram positive (S. aureus) bacteria. The bacteria's were prepared at Adama Science and Technology university of Biology department,Ethiopia .Antibacterial activity test was conducted by agar well diffusion method. We measured our nanocomposite on two different weights starting from the most frequently used weight of 15mg/ml and 20mg/ml. The measured nanocomposites are dispersed in the DMSO (Dimethyl Sulfoxide) for 30minute.Then three wells are formed on the medium. The prepared nancomposite solution was added in the drilled part of the media and incubated at 35 ^{0}C for 24hrs. After 24hrs zone of inhibition we measured for 15mg/ml nancomposites. We had faced a difficulty on measuring the value of 20mg/ml nanocomposite due to its high inhibition of the bacteria's. As shown in table 1, inhibition zone of nanocomposite is better in gram positive (S. aureus) as compared with gram negative (E. coli) bacteria because of Gram-negative bacteria (E. coli) typically contain thin cell wall and outer cell. Gram-positive bacteria contain a thick layer of cell wall as membrane layer of cytoplasmic membrane. This outer membrane well. This makes gram-positive bacteria more susceptible to resists certain drugs and antibiotics from penetrating the bacteria antibiotics than gram-negative bacteria1 due to gram positive

bacteria had thick cell wall which leads to absorb nanocomposite highly compared to gram negative bacteria [21]. In this work, antibacterial activity from amorphous silica supported CuO/ZnO shows 59.1% on S.aureus and 63% on E.coli compared with CuO/ZnO bare, also 57% on S. aureus and 60% on E.coli compared with crystalline silica supported CuO/ZnO. This is due to porous nature of amorphous silica which promotes the growth of CuO/ZnO hairy like structure as confirmed by SEM. This in turns leads to increase surface area of amorphous silica supported CuO/ZnO provides large surface area and high generation of ROS which leads to more inhibition of bacteria.

Samples	Staphylococcus aureus	Escherichia coli
CuO/ZnO bare	25 mm	15 mm
CuO/ZnO grown on Amorphous silica	37.1 mm	26.3mm
CuO/ZnO grown on Crystalline silica	27mm	17.5 mm

Table 1: Zone of inhibition in mm

4. Conclusion:

Three samples: CuO/ZnO bare, amorphous silica supported CuO/ZnO and crystalline silica supported CuO/ZnO were successfully synthesized by sol- gel method and then the antibacterial activities of three nanocomposites have compared on gram-negative (E.coli) and gram-positive (S. aureus) bacteria. The calculated crystal sizes from XRD data are 16.3 nm for CuO/ZnO bare, 12.5 nm for amorphous silica supported CuO/ZnO and 29.1 nm for crystalline silica supported CuO/ZnO. In addition, this, the hairy like structure of CuO/ZnO nanocomposite were seen on amorphous silica supported CuO/ZnO by using SEM. When antibacterial activities of three nanocomposites were tested by using the agar diffusion method, amorphous silica supported CuO/ZnO showed inhibition zone of 59.1% for S. aureus and 63% for E.coli compared with CuO/ZnO bare, also 57% for S.ureus and 60% for E.coli compared with Crystalline silica supported CuO/ZnO. Therefore, amorphous silica supporting CuO/ZnO nanocomposite is a promising antibacterial agent.

Acknowledgments:

The authors are grateful to the Department of Materials Science and Engineering Adama Science and Technology University for supporting and encouraging us during this article has been developed.

References:

1. Nabila, M. I., & Kannabiran, K. (2018). Biosynthesis, characterization and antibacterial activites of copper oxide nanoparticles (CuO NPs) from actinomycetes. Biocatalysis and gricultural biotechnology, 15, 56-62
2. Bratovcic, A. (2019). Different applications of nanomaterials and their impact on theEnvironment. SSRG International Journal of Material Science and Engineering, 5(1).
3. Yang H, Tao Q, Zhang X, Tang A, Ouyang J. (2008). Solid-state synthesis and electrochemical property of SnO2 /NiO nanomaterials. J. Alloy Compd. 459, 98–102.
4. Fang J, Ma J, Sun Y, Liu Z, Gao C, (2011). Electrochemical synthesis of nanocrystalline SrNb2O6 powders and characterization of theirphotocatalytic property. Mater. Sci. Eng. B, 176, 701–705.
5. Gold, K., Slay, B., Knackstedt, M., & Gaharwar, A. K. (2018). Antimicrobial activity ofmetal and metal-oxide based nanoparticles. Advanced Therapeutics, 1(3), 1700033.
6. Sun, J. H., Dong, S. Y., Wang, Y. K., & Sun, S. P. (2009). Preparation and photocatalytic property of a novel dumbbell shaped ZnO microcrystal photocatalyst. Journal of Hazardous Materials, 172(23), 1520-1526.
7. Manyasree, D., Peddi, K. M., & Ravikumar, R. (2017). CuO nanoparticles: synthesis, characterization and their bactericidal efficacy. Int J ApplPharmaceut, 9(6), 71-74.
8. Nandiyanto, A. B. D., Zaen, R., & Oktiani, R. (2017). Correlation between crystallite size and photocatalytic performance of micrometer sized monoclinic WO3 particles. Arabian Journal of Chemistry.
9. Bandara, J., Hadapangoda, C. C., & Jayasekera, W. G. (2004). TiO2/MgO composite photocatalyst: the role of MgO in photoinduced charge carrier separation. Applied Catalysis B: Environmental, 50(2), 83-88.
10. Ahmmad, B., Leonard, K., Islam, M. S., Kurawaki, J., Muruganandham, M., Ohkubo, T., & Kuroda, Y. (2013). Green synthesis of mesoporous hematite (α-Fe2O3) nanoparticles and their photocatalytic activity. Advanced Powder Technology, 24(1), 160- 167.
11. Qiu, S., Zhou, H., Shen, Z., Hao, L., Chen, H., & Zhou, X. (2020). Synthesis, characterization, and comparison of antibacterial effects and elucidating the mechanism of ZnO, CuO and CuZnO nanoparticles supported on mesoporous silica SBA-3. RSC Advances, 10(5), 2767-2785.
12. Mengistu, T. (2018). Synthesis and Characterization of Zeolite A Using Bagasse Ash, as Bio Silica Source for Water Hardness Removal (Doctoral dissertation, ASTU).
13. Rahman, N., Sabali, M. A., Sandu, A. V., Sahiron, N., & Sandu, I. G. (2016). Study Of calcination temperature and concentration of NaOH effect on crystallinity of silica from sugarcane bagasse ash (SCBA). Revista De Chimie-Bucharest, 67(9),1872-75.
14. Widiarti, N., Sae, J. K., & Wahyuni, S. (2017, February). Synthesis CuO-ZnO nanocomposite and its application as an antibacterial agent. In IOP Conference Series: Materials Science and Engineering.
15. Arunkumar, B., Jeyakumar, S. J., &Jothibas, M. (2019). A sol-gel approach to the synthesis of CuO nanoparticles using Lantana camara leaf extract and their photocatalytic activity. Optik, 183, 698-705.
16. Shen, Z., Zhou, H., Chen, H., Xu, H., Feng, C., & Zhou, X. (2018). Synthesis of nano-zinc oxide loadedOnmesoporous silica by coordination effect and its photocatalytic degradation property of methyl orange. Nanomaterials, 8(5), 317.
17. Tanaka, K., Capule, M. F., &Hisanaga, T. (1991). Effect of crystallinity of TiO2 on its photocatalyticaction.Chemical Physics Letters, 187(1-2), 73-76.
18. Sakib, Abdullah Al Mamun, et al. (2019)."Synthesis of CuO/ZnONanocomposites and Their ApplicationInPhotodegradation of Toxic Textile Dye."

Journal of Composites Science 3.3: 91.

19. Elfeky, Ahmed S., et al. (2020). "Multifunctional cellulose nanocrystal/metal oxide hybrid, photo-degradation, Antibacterial and larvicidal activities." Carbohydrate Polymers 230: 115711.
20. Gondal, M. A., et al. (2009) "Synthesis of ZnO2 nanoparticles by laser ablation in liquid and their annealing transformation into ZnO nanoparticles." Applied surface science256.1298- 304.
21. Zeng, X., & Lin, J. (2013). Beta-lactamase induction and cell wall metabolism in Gram-negative bacteria.Frontiers in microbiology, 4, 128. 21.